Biological Nanopores for Single-Molecule Biophysics

Manuscript received: 21/08/2009; Article published: 24/11/2009

Biological Nanopores for Single-molecule Biophysics**

Long Ma and Scott L. Cockroft *

EaStCHEM, School of Chemistry, Joseph Black Building, University of Edinburgh, West Mains Road, Edinburgh, EH9 3JJ, UK.

[*]Corresponding author; e-mail: scott.cockroft@ed.ac.uk, tel: +44 (0)131 650 4758

[**]Financial support is graciously acknowledged from the Chinese Scholarship Council and the MTEM International Studentship scheme (scholarship to L. M), The Royal Society of Chemistry and The Leverhulme Trust. We thank J. Chu of the Ghadiri laboratory (The Scripps Research Institute) for helpful discussions.

Graphical abstract:

Keywords:
bionanotechnology;biosensors;nanopores;single-molecule biophysics;supramolecular chemistry

Abstract

Single-molecule methods have revolutionised the way that biological questions are tackled. Contributions to the field of biophysics from biological nanopore-based methods are reviewed.

1. Introduction

Single-molecule methods have revolutionised the way that biological questions are tackled.[1, 2] Single-molecule techniques can resolve the distribution and temporal order of events including transient intermediates, pauses, multiple pathways, and even reverse steps that would otherwise be obscured in ensemble studies. By observing one molecule at a time, the averaging of signals from an ensemble of many molecules can be avoided to reveal the distribution and individual dynamics of sub-populations. In the 15 years since nanopore detection first emerged the method has established itself as a sensitive complementary technique for examining biological interactions at the single-molecule level. A wide range of analytes have been examined including; nucleic acids, peptides, and polymers.[3, 4] The breadth of these applications is ever expanding, helped by the fact that biological nanopores can be engineered using modern chemical and biological techniques to tune their suitability to a particular application. For example, there continues to be much excitement surrounding the application of nanopore-based methods for sequencing DNA on the single-molecule level.[5, 6] Although recent advances in nanofabrication techniques have expanded the field to include man-made solid-state nanopores,[7] this review will focus on the application of single-molecule methods that exploit the nanometre dimensions of the α-haemolysin protein pore for studying the structure, activity and interactions of biomolecules.

2. Background

2.1 The α-haemolysin nanopore

α-haemolysin (αHL) is toxin protein secreted by the pathogen *Staphylococcus aureus* as a 33.2 kDa water-soluble monomer. αHL monomers spontaneously self-assemble in phospholipid bilayers to form heptameric mushroom-shaped protein pores (Figure 1).[8] αHL displays its exotoxic activity by binding to, and forming transmembrane channels in a wide range of mammalian cells including erythrocytes, lymphocytes and endothelial cells.[9] The cap opening is approximately 26 Å in diameter and leads into a larger inner vestibule. A 15 Å diameter constriction connects this vestibule to the *β*-barrel transmembrane stem, which consists of 14 antiparallel strands and has an internal diameter of 22 Å.

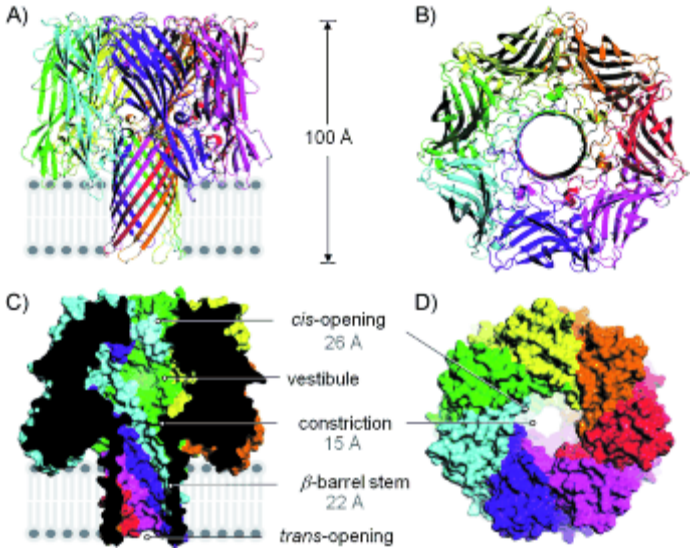

Figure 1. A) Side view of the α-haemolysin heptameric complex showing the approximate location of the lipid bilayer (αHL, PDB ID: 7AHL).[9] The complex is ~100 Å in both height and diameter. B) View of α-haemolysin from the *cis*entrance to the pore. C) and D) Cross-sectional and space-filling models of α-haemolysin showing the internal diameter of the pore channel at different locations. Each colour represents a different α-haemolysin monomer subunit.

2.2 The principle of single-molecule nanopore detection

αHL can serve as a detection element for examining single-molecules. In a typical experimental setup, a thin insulating polymer sheet containing a small aperture (between 50-1000 □m in diameter) is sandwiched between two wells containing an electrolyte buffer.[10] A planar lipid bilayer membrane is then formed in this aperture, either by 'painting' lipid over the aperture,[11] or by lowering and raising a lipid monolayer floating on the surface of the buffer solution over the aperture opening.[12] Each electrolyte chamber contains an electrode connected to a patch-clamp amplifier, a piece of equipment that earned Erwin Neher and Bert Sakmann the Nobel Prize for Physiology or Medicine in 1991 for their pioneering work in the field of electrophysiology.[13] [14] Since a lipid bilayer is electrically insulting, no electrical current can flow between the two electrolyte chambers when a bilayer is formed (a GΩ membrane resistance can be obtained routinely). A trace amount of αHL is then added to either of the electrolyte chambers. Pore insertion into the suspended membrane is a stochastic event and can take anything from a few seconds to several hours to occur, which often requires much patience on the part of the researcher! In favourable circumstances, then a state where a *single* protein channel is inserted in the membrane can be obtained as shown in the generic experimental set-up shown in Figure 2. Under these conditions and upon the application of a transmembrane potential difference (voltage), a stable measurable electrical current arises from the passage of ions through the

channel pore (Figure 2A). Analyte molecules may modulate the ionic current flowing through the protein channel. For example, a large molecule passing through the pore will reduce the magnitude of the ionic current more than a smaller molecule. Thus, the current signature (Figure 2B) obtained from a single-channel current recording can be used to identify single molecules from the distribution, duration and ordering of events. Due to the random nature of events occurring on the single-molecule level, the approach is sometimes referred to as 'stochastic sensing'.[3],[16]

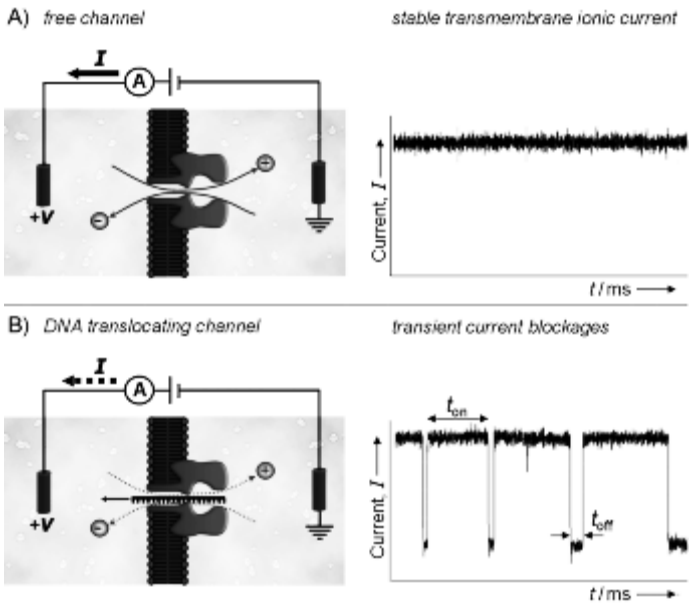

Figure 2. A platform for single-molecule experiments. Experimental setup with a single α-haemolysin protein pore embedded in a suspended phospholipid bilayer. A) When a transmembrane voltage (V) is applied across the bilayer, a stable current (I) arises from the passage of ions through the pore channel. B) Transient ionic current blockades corresponding to the translocation of negatively charged single-stranded oligonucleotides through the nanopore.[16] The duration of the translocation (dwell time), t_{off}, and the inter-event duration, t_{on}, are indicated. Since the average frequency of the current blockades is proportional to the concentration of the analyte [c], the method gives direct access to the rate constant of capture/association ($k_{on}=1/t_{on}[c]$), and the rate constant of translocation/dissociation, ($k_{off}=1/t_{off}$).

3. Manipulation and recognition of nucleic acids using nanopores

Single oligonucleotide molecules have been examined using a wide range of methods such as atomic force microscopy, fluorescence microscopy, and optical tweezers.[2] Distinct from other single-molecule methods, nanopore detectors facilitate the direct investigation of oligonucleotides without

the need for chemical modifications, amplification, or attachment to a solid surface. Nonetheless, chemical modification of the analytes and the use of engineered protein pores further broadens the utility of the approach. Taken together, these approaches are able to provide insight into the sequence, structural dynamics and thermodynamics of oligonucleotide primary, secondary and tertiary structures.

3.1 Structure and hybridisation recognition in unmodified oligonucleotides

Kasianowicz and co-workers were the first to demonstrate that single-stranded RNA and DNA molecules can be driven through a single αHL nanopore by the electric field created upon the application of a transmembrane potential difference (voltage) (Figure 2B).[2, 15] The transient ion current blockages resulting from the passage of oligonucleotides through the pore channel were used to measure the length of oligonucleotides since the duration of passage of each molecule was proportional to the length of the polymer. Using this pioneering methodology, Meller and co-workers were able to calculate the speed of DNA translocation through the pore.[6] Polymers longer than the length of the pore translocated at an average constant velocity, whilst the translocation speed of shorter polymers increased with decreasing length. The speed of translocation increased non-linearly as the transmembrane potential was increased.

In subsequent work, the approach was extended to investigate different DNA block co-polymers using more advanced signal analyses.[16] The translocation of each polymer gave unique distributions of the translocation duration and blockage currents, which could then be used to distinguish between different 100-mer DNA block co-polymers in a mixed sample. The temperature dependence of the event characteristics suggested that the distinguishing features of different oligonucleotides arose from the secondary structures of the oligonucleotides studied.

As we have seen, the lumen of the wild-type αHL is wide enough to accommodate the translocation of single-stranded oligonucleotides. Although dsDNA is too large to translocate the pore, it can be trapped within the wide lumen on the *cis*-side of the pore (see vestibule in Figure 1C). This has been exploited to inspect the unzipping kinetics of individual DNA hairpins under constant force and constant loading rate (Figure 3).[17] By employing real-time dynamic voltage control, the applied voltage pattern could be tuned to control the rate of DNA unzipping and subsequent translocation through the pore. The unzipping times decreased exponentially with the voltage giving a characteristic slope that was independent of the duplex region sequence. The magnitude of the voltage required to achieve almost instantaneous unzipping upon DNA capture (Figure 3B→D) was found to depend strongly on the stability of the duplex region. In an extension of this work, unzipping of dsDNA was achieved under an applied transmembrane potential as before (Figure 4A→B). Polymerase chain

reaction (PCR) analysis of the DNA content of the solution on both sides of the bilayer proved that only one of the two DNA strands was pulled through the protein pore (Figure 4C). The ionic current blockage of polynucleotide traversal revealed information about the time-scale of DNA unzipping events. Furthermore, a simple kinetic model was used to estimate the unzipping enthalpy barriers and the effective charge of the nucleotides within the pore lumen.

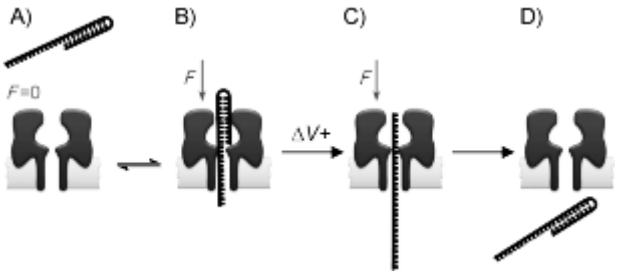

Figure 3. A) to B) Single-stranded DNA hairpin capture. C) to D) Application of an increased transmembrane voltage causes the DNA to unzip and translocate through the pore.

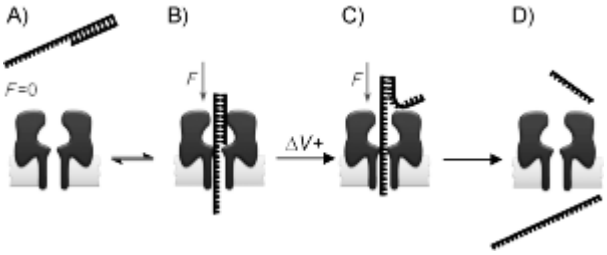

Figure 4. A) to B) Capture of double-stranded DNA with a single-stranded overhang. C) to D) Subsequent unzipping of DNA induced at higher transmembrane voltages. Only the longer ssDNA strand was seen to translocate the pore upon unzipping.[17–20]

G-quadruplexes are tertiary DNA structures that form in guanine-rich nucleotide sequences identified in numerous gene promoter sequences and within telomeric DNA. As such, they are potential drug targets for cancer and other genetic diseases.[23] Gu and co-workers have explored the activity of cations in regulating the folding and unfolding of the G-quadruplex formed by the thrombin-binding aptamer (GGTTGGTGTGGTTGG) using the nanopore approach (Figure 5A).[21] The nanopore current signature showed that G-quadruplex formation is cation-selective, and the order of the ability of ions to stabilise G-quadruplex was found to be $K^+ > NH_4^+ \sim Ba^{2+} > Cs \sim Na^+ > Li^+$. G-quadruplex was not detected in the presence of Mg^{2+} and Ca^{2+}.

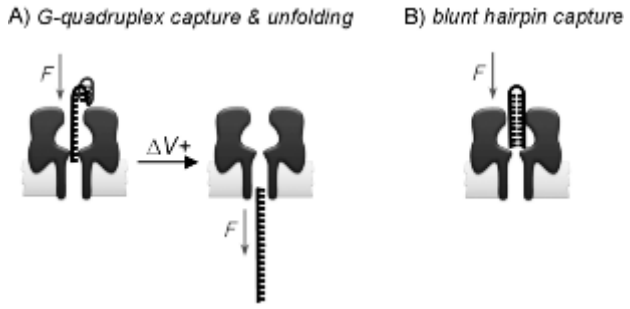

Figure 5. A) DNA G-quadruplex capture, unfolding and channel translocation under a driving potential.[22] B) Ion current signals can be used to identify Watson–Crick base pairs, mismatches and unnatural base pairs at the termini of single, blunt DNA hairpin molecules captured within a nanopore.[18, 19, 23]

3.2 Sequence recognition in unmodified oligonucleotides

There has been an increasing focus on DNA sequencing by single-molecule methods since the completion of the Human Genome Project. Advances in sequencing techniques are expected to help to achieve large-scale, systematic sequencing of cancer genomes, unravel the genetic basis of disease and guide the development of personalised healthcare.[24] To achieve this grand aim, time- and cost-efficient sequencing methods are required. Nanopore-based methods offer some promise in this regard because the restricted size of a nanopore channel ensures that the native order of the nucleotides is retained as a strand of DNA threads through the nanopore. It was proposed that kilobase-length single-stranded genomic DNA could be threaded through the pore, and its sequence revealed by the ionic current signals without the need for fluorescent labels or amplification.[5]

Early investigations of oligonucleotide recognition using αHL found that polycytidylic (polyC), polyadenylic acid (polyA), and polyuridylic acid (polyU) RNA homopolymers could be characterised using ion current amplitudes and dwell times.[25] In addition, the approach could distinguish between polyC and the polyA segments within a single RNA molecule. When A_{50} and C_{50} passed through the nanopore, different current levels were observed. Similarly, when RNA block co-polymers $A_{25}C_{50}$, $C_{50}A_{25}$, $A_{25}C_{50}$ and $C_{50}A_{25}$ passed through the nanopore, two distinct current levels were observed within each translocation event that corresponded to the A and C regions in each molecule.[26] It was also possible to identify the orientation of oligonucleotides as they translocate through a single αHL pore (3'-leading *vs.* 5'-leading). 3'→5' translocation of polyC RNA through αHL resulted in a significantly higher current blockage compared with 5'→3' translocation, and threading was preferred from the 3'-end compared to the 5'-end. Similarly, when capturing ssDNA hairpins (Figure 4A to 4B), the residual current ($I_{DNA}/I_{free\ channel}$) for 3'→5' ssDNA threading from the *cis*-side was lower

compared with 5'→3' threading (9% *vs.* 12% respectively).[27] Voltage-driven 3'→5' capture from the *cis*-side of the pore was also faster than 5'→3' capture. Interestingly, escape from the pore under zero applied potential was slower for 5'→3' unthreading than in the opposite direction (Figure 4B to 4A). Molecular dynamics simulations suggested that base tilting during threading may have been the origin of this difference.

Ghadiri and co-workers have pushed oligonucleotide recognition using unmodified αHL to its limits by demonstrating recognition of a single base in an ssDNA molecule. This was achieved by capturing DNA hairpins on the *cis*-side of an αHL pore under an applied electric field (Figure 3B). Initially, DNA hairpins with different polyA or polyC segments were discriminated using ion currents. After extensive optimisation of the hairpin designs, it was found that a single adenosine base could be distinguished from cytosine at a specific position within a region of polyC ssDNA.[28] To date, this study still represents the closest that anyone has come to reading the sequence of unmodified ssDNA using wild-type αHL ion current recordings.

Discrimination among individual Watson-Crick base pairs at the termini of single DNA and RNA hairpin molecules has also been investigated using single nanopores (Figure 5B). Hundreds of hairpin molecules could be examined, classified and quantified in a few minutes, and revealed that it was possible to resolve single-nucleotide and single-base pair differences between otherwise identical DNA hairpin molecules.[22] Computational pattern analysis of ion current recordings enabled each of the different combinations of Watson-Crick base pairs and their orientation to be identified.[18, 19] The work was extended to examine the behaviour of terminal base pairs upon substitution of thymine for the unnatural base fluorotoluene. Kinetic analysis suggested that the characteristic signals caused by each of the different combinations of base-pairs were dependent on the stability of the terminal base pair and its nearest neighbour.

Clearly, there have been many impressive examples of direct recognition of unmodified oligonucleotides. However, a practical nanopore-based method for sequencing unmodified DNA using αHL remains elusive. Two barriers to this aim are the rapid translocation speed of unmodified oligonucleotides and the fundamental limitations of ion current recognition. This has motivated researchers to explore alternative avenues of nanopore research, particularly those that exploit modified oligonucleotides and engineered nanopores.

3.3 Exploitation and recognition of modified oligonucleotides

Advances in automated synthesis, chemical, and biochemical methods provide access to a plethora of oligonucleotide modifications with an extensive range of applications that span the physical,

biological and medical sciences.[29] Such modified oligonucleotides have provided new opportunities for expanding the capabilities of αHL sensing technologies.

One frequently employed oligonucleotide modification is biotinylation. Single biotinylated oligonucleotides can be captured within a nanopore when capped with avidin/streptavidin proteins (Figure 6A to 5B). These proteins are too large to translocate the pore and thus serve as 'stopper' and allowing the read-time of current recordings to be increased. PolyA, polyC and polyT ssDNA co-polymers captured in this way could be distinguished from each other due to their distinct ion currents.[8] As in earlier studies, ion current blockages were found to be orientation dependent, giving different currents when threaded from the 3'- or the 5'-direction. The different homopolymers could be distinguished most easily when threaded from the 5'-end. In a recent *tour de force* study, Bayley and co-workers systematically scanned the recognition of streptavidin-capped ssDNA strands captured within wild-type and mutant αHL pores.[31]

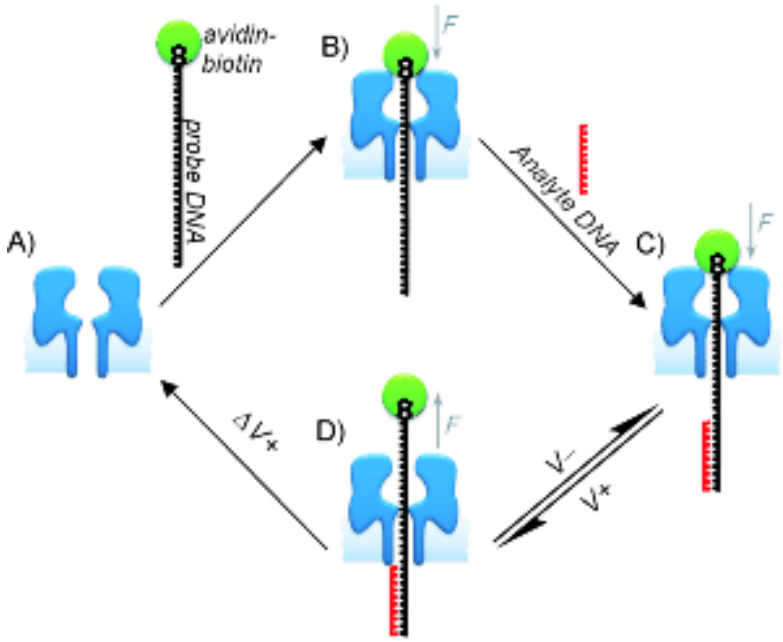

Figure 6. A nanosensor for sequence-specific detection of an ssDNA analyte across a bilayer. A)→B) A biotinylated DNA probe with a terminal avidin anchor is captured within a nanopore under an applied transmembrane potential. The 3′-end of the DNA probe is exposed on the *trans* side of the pore. B)→C) When the analyte DNA is present, it can specifically bind to the protruding complementary single-stranded DNA probe to furnish a fully interlocked αHL·DNA rotaxane complex. C)→D) The position of the threaded strand can be flipped back and forth by changing the sign of the applied potential. D)→A) Higher potentials force the analyte DNA to dissociate from the probe DNA and free the pore.[30]

Independent studies arising from both the Marziali and the Ghadiri laboratories took advantage of this 'stoppering' approach to form DNA 'rotaxanes' of transmembrane pores (Figures 5 to 7).[30, 32] A rotaxane is a mechanically-interlocked molecular architecture formed when one molecule is threaded through the centre of another ring-shaped molecule. In this case, the thread is the ssDNA, the ring is the αHL protein pore, and the stoppers are avidin/streptavidin and dsDNA.[33] Trapping the threaded DNA in this manner facilitates multiple ion current readings of the same DNA molecule.

Marziali used such a device to study the relationship between duplex dissociation time and DNA hybridisation energy at the single-molecule level.[30] The ssDNA probe contained a specific recognition sequence at the 3'-end, and a biotin modification at the 5'-end bound to an avidin stopper. By applying a transmembrane potential, the ssDNA conjugate was threaded through the pore, exposing the 3'-end of the DNA probe on the opposite side of the membrane (Figure 6A to 5B). When captured in this way, the probe sequence was free to bind a complementary oligonucleotide sequence and form a rotaxane complex (Figure 6C).[34] Reversal of the applied potential made the DNA probe withdraw from the pore (Figure 6D), and under a high enough potential, this force caused the analyte DNA sequence to dissociate from the DNA probe (Figure 6D to 5A). The time required for DNA unzipping could be used to identify different oligonucleotides and single-base mismatches.

In Ghadiri's variation of the rotaxane approach (Figure 7), DNA-PEG co-polymers were trapped within the pore using a streptavidin stopper on one side of the membrane and a dsDNA stopper on the other. As before, the position of the DNA-PEG co-polymer could be flipped back and forth by changing the sign of the transmembrane potential, but this time, different ionic currents were recorded depending upon whether the DNA or the PEG segments of the co-polymer were occupying the pore channel. The smaller cross-section of PEG means that it blocks the ionic current flowing through the pore less than an oligonucleotide (Figure 7).[32]

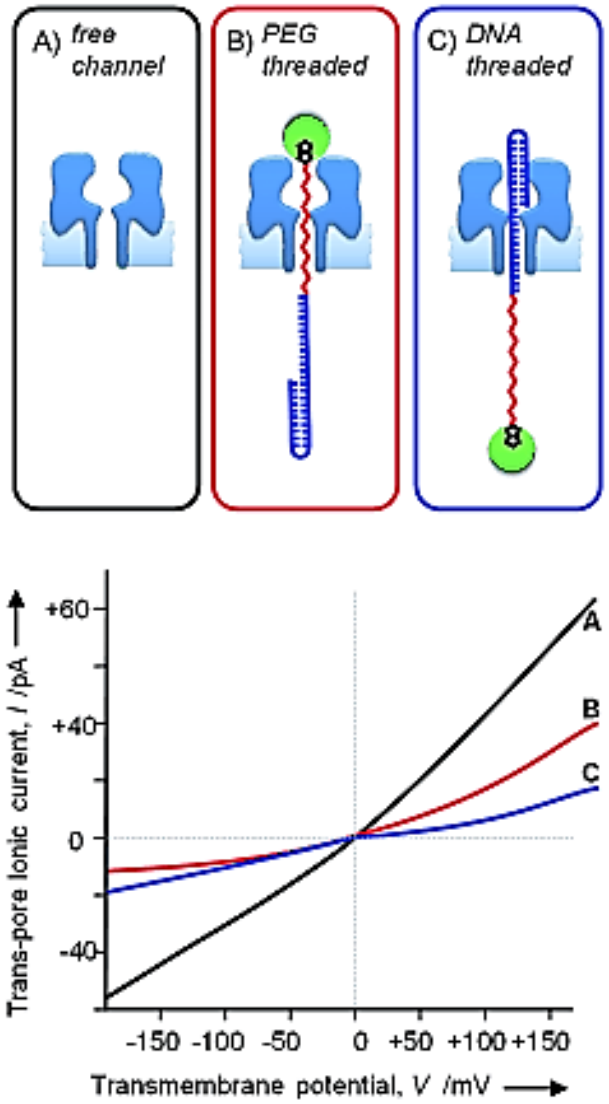

Figure 7. DNA–PEG co-polymer rotaxanes assembled with dsDNA and biotin–streptavidin stoppers. Distinct current–voltage (*I*–*V*) traces were obtained depending on the direction of threading through the pore.[32]

This simple recognition between PEG and DNA was extended in later work by carefully tuning the length of the DNA and PEG regions such that the small changes in the proportion of DNA to PEG would result in a change in the ionic current flowing through the pore (Figure 8).[35] The approach was sufficiently sensitive to allow the length of the double-stranded DNA region to be measured with single-base precision over a 10-base reading window. Further analysis of the signal-to-noise ratios revealed an maximum spatial resolution of 1.4 Å. Later, this supramolecular device was used to monitor DNA polymerase-catalysed nucleotide extension with unprecedented single-base resolution at the single-molecule level (see Figure 15).

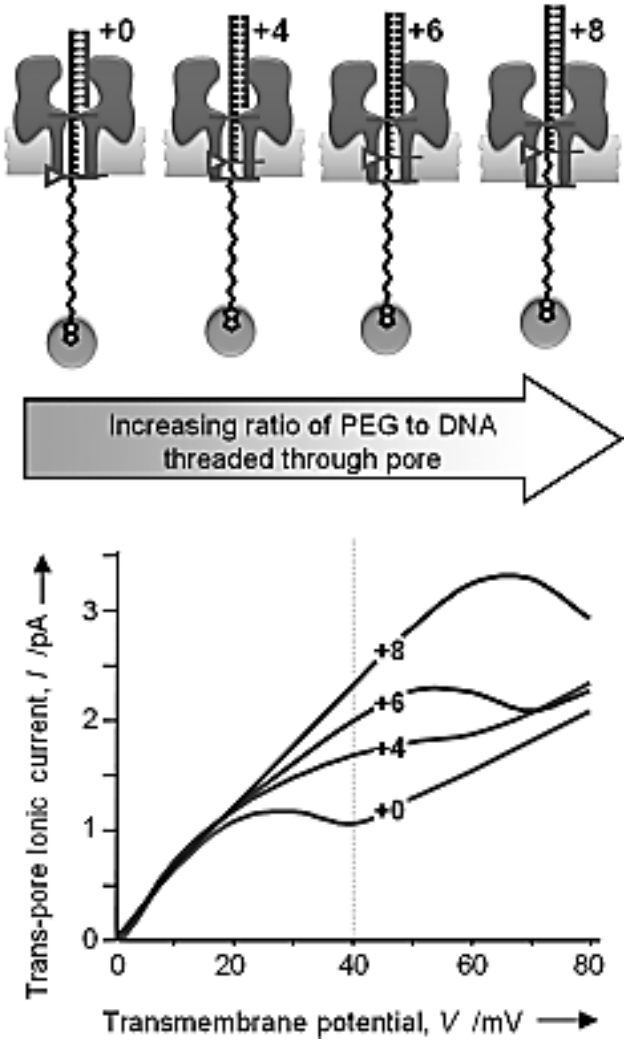

Figure 8. Supramolecular nanopore-based device that can measure the length of a single molecule of DNA with ångström-scale resolution. Variation of the length of the dsDNA duplex region (+0 to +8 bases) changes the proportion of DNA to PEG threaded through the β-barrel of the αHL pore. The differences in the length of the coloured DNA molecule manifest themselves in the characteristic current–voltage (*I*–*V*) trace of each complex. The largest and most reproducible current difference between the four complexes was obtained at +40 mV (vertical grey dotted line).[35]

Recently, Howorka and Mitchell chemically modified ssDNA with a peptide tag. This increased the cross-sectional diameter of the DNA, and was found to slow down the speed of translocation through the pore (Figure 9A). The current signatures of peptide-tagged DNA depended on the length, charge and size of the tag. This facilitated the identification of up to two different bases during the translocation of a single strand of DNA.[36]

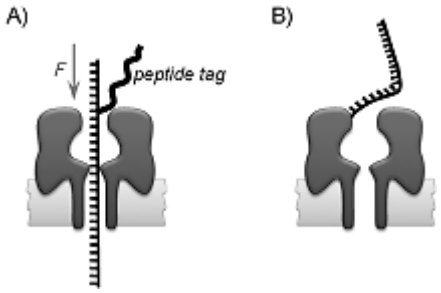

Figure 9. A) Translocation of an ssDNA molecule tagged with a peptide.[36] B) Modified αHL pore with an ssDNA sequence attached to a mutant cysteine residue.[37, 38]

3.4 Recognition of mononucleotides using engineered nanopores

One of the major advantages of biological nanopores such as αHL, is that the protein sequence can be readily engineered using molecular biology and subsequently chemically modified.[39, 40]. For example, a short ssDNA was tethered to the genetically modified heteroheptameric αHL pore to form a 'DNA-nanopore' biosensor (Figure 9B). The DNA-nanopore was able to distinguish between complementary individual DNA strands of up to 30 nucleotides in length that only differed by a single base.[37, 38]

Bayley and co-workers have also pioneered the use of so-called 'molecular adapters' such as cyclodextrin to enhance the recognition properties of αHL (Figures 10 and 11).[39] This approach allows analytes that would normally be too small to be recognised by wild-type αHL to be detected upon binding to the molecular adaptor lodged within the αHL channel. Recently, αHL mutants have been engineered to enhance the stability of the adapter•αHL complex. By using a mutant $(M113R)_7$ nanopore equipped with a heptakis-(6-deoxy-6-amino)-*β*-cyclodextrin adapter it was possible to distinguish between each of the four different ribonucleosides and 2'-deoxyribonucleoside 5'-monophosphates (rNMPs and dNMPs).[40] NMPs could only be identified when the cyclodextrin adapter was bound in the pore. However despite the use of mutant pores, the adapter was only transiently bound within the pore (Figure 10B). This limitation was overcome by engineering a nanopore with a covalently attached cyclodextrin adapter to achieve a continual read-out at a high data acquisition rate (Figure 11).[41] The sensor was capable of detecting deoxynucleotide 5'-monophosphate molecules with an accuracy of 99.8%, and was even able to discriminate methylated cytosine 5'-monophosphates from the standard DNA bases.

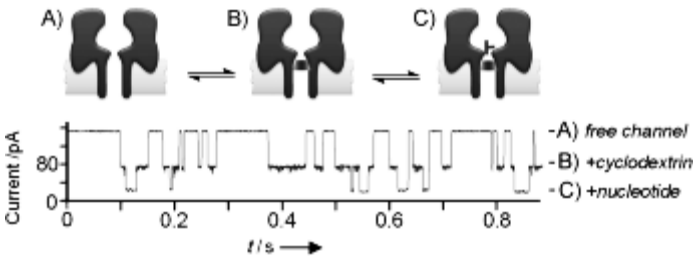

Figure 10. Single-channel ionic current recordings showing nucleotide monophosphate recognition with a cyclodextrin nanopore adapter. A) Free channel (open pore). B) αHL nanopore with a noncovalently bound cyclodextrin adaptor. C) Subsequent binding and recognition of a nucleotide monophosphate.[39]

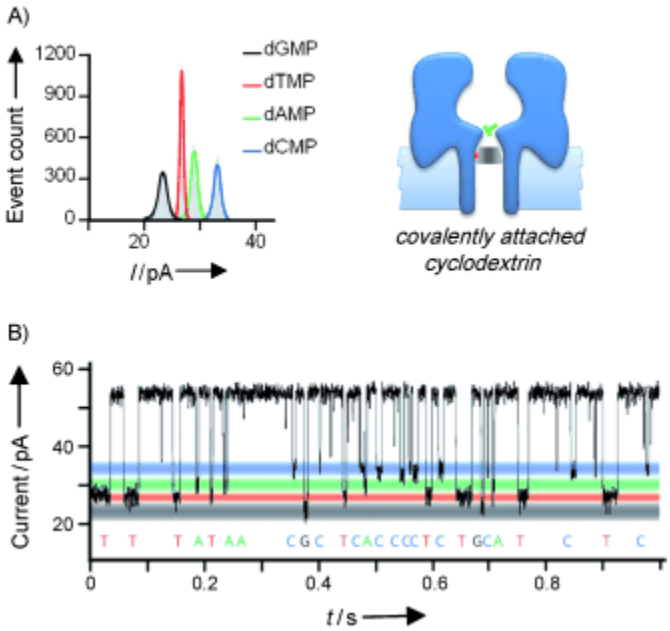

Figure 11. A) Gaussian fits of current histograms corresponding to dGMP, dTMP, dAMP and dCMP recognition by an engineered nanopore with a covalently attached cyclodextrin adapter.[40] B) Single-channel recording from the permanent adapter nanopore displaying real-time recognition of discrete dGMP, dTMP, dAMP and dCMP current levels.

It has been proposed that this approach could be developed as a novel method of DNA sequencing if used in combination with an exonuclease that processively cleaves mononucleotides one-by-one from the end of an ssDNA chain. In a step towards this aim, it was shown that highly accurate dNMP recognition was maintained under experimental conditions compatible with the exonuclease EcoExo I. At high potential (+180 mV) the dNMPs passed directly through the pore after being read, meaning

that erroneous duplicated reads of the same dNMP molecule can be avoided. Nevertheless, several other problems must be solved before this approach can be adopted as a viable technique for DNA sequencing. Above all, each dNMP molecule must enter the nanopore in the same sequence that they are cleaved by the exonuclease.

4. Investigation of peptides and proteins using nanopores

The structure and function of peptides and proteins are intimately related, and only certain conformations may exert biological activity. In this section, nanopore approaches for investigating the structure, interactions, and activity of peptides, proteins and nucleic acid-manipulating enzymes will be described.

4.1 Probing the structures of peptides and proteins

The nanopore approach can be used as a tool to gain insight into the structure of peptides. Lee, Kraatz and co-workers synthesised peptides containing one, two, or three, repeats of the collagen-like sequence $(Gly\text{-}Pro\text{-}Pro)_n$ bearing positively charged ferrocene units at each end.[42] Circular dichroism (CD) spectra suggested that the peptide forms a triple helix when n = 3, a double-helix when n = 2, and has no dominant secondary or tertiary structure when n = 1. When these charged peptides were driven through the nanopore (Figure 12A), each peptide generated a unique blockage current *vs.* translocation duration fingerprint. The triple helix gave the largest current blockage and dwell times, while the double helix and the monomer gave rise to smaller current blockages and shorter dwell times. Importantly, the nanopore analysis revealed the presence of intermediate conformations that could not be detected using bulk spectroscopic techniques, such as CD or NMR, highlighting one of the major advantages of single-molecule methods.

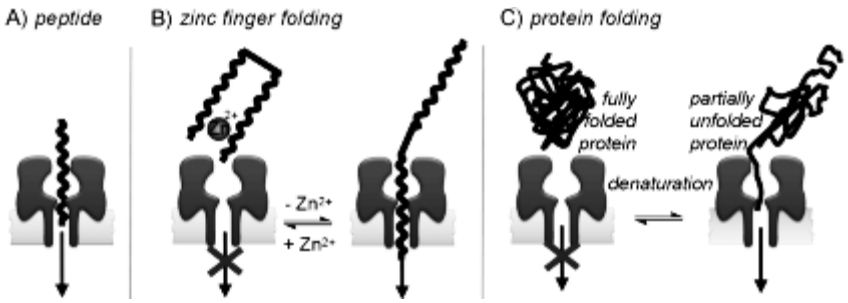

Figure 12. Structural analysis of A) simple peptides,[42–44] B) zinc fingers[45] and C) protein folding by using nanopores.[46]

Taking this one step further, the nanopore technique can also be used to study the folding and unfolding of proteins and peptides at single-molecule level. Lee and co-workers used the nanopore method to examine folding in Zif168, a zinc finger containing 28 amino acids (Figure 12B). In the folded state, Zif168 contains *β*-sheet, α-helix, and turn motifs, and is too large to enter the lumen of αHL. Meanwhile, in the absence of Zn^{2+} ions the peptide is unfolded and is able to translocate the pore.

Current signature analysis in the absence of Zn^{2+} revealed two different populations, which were attributed either bumping (with small ion current blockages and long dwell times) or translocation events (with large ion current blockages and short dwell times).[45] Upon addition of an equimolar concentration of Zn^{2+}, the ratio of translocation events to bumping events decreased. Further work examined the unfolding of an 86-residue protein as it translocated the αHL nanopore, establishing the generality of the approach for studying the conformations of peptides and small proteins.[47] Remarkably, it was found that a single mutation to the 86-residue protein was sufficient to dramatically change the blockage event profiles, demonstrating the sensitivity of this nanotechnology to structural changes in biomolecules. In the ultimate extension of this work, Pelta and co-workers examined the guanidinium-induced unfolding of the 370-residue (40 kDa) maltose binding protein (MBP) (Figure 12C).[46] In absence of the guanidinium, the native MBP protein could not enter the αHL pore, and no blockage events were observed. However, many current blockages emerged after the addition of 1.35 M guanidinium hydrochloride. The ion current traces revealed partially folded conformations, as evidenced by longer duration blockages at lower concentrations of guanidinium hydrochloride.

4.2 Studying protein-binding interactions

In addition to probing the underlying biophysics of nanopore translocation, αHL has served as a convenient model for studying the interactions of proteins and peptides with membrane-spanning *β*-barrels. Furthermore, modified αHL pores featuring specific binding sites have enabled to the investigation of specific protein binding interactions.

Lee, Kraatz and co-workers synthesised a collection of negatively charged α-helical peptides and characterised their translocation through both αHL (Figure 12A).[43] The ratio of bumping to translocation events was related to the charge and dipole moment of the peptide in addition to the applied transmembrane potential. It was suggested that larger dipoles and electric fields facilitate the alignment of the peptide with the pore channel. Weaker fields and peptides with neutral charge or low-dipole moments were less likely to align with the pore channel, increasing the likelihood of bumping events. Furthermore, threading from the *cis*-side of the pore was favoured over threading

from the trans-side, suggesting that the vestibule helps to align and funnel the peptides through the channel. For translocation events, both the ion current blockage and the blockage duration increased with the length of the peptides.[43] These results mirrored the work of Movileanu and co-workers, who found similar results for the translocation of cationic peptides through αHL channels.[44]

It has been suggested that the hydrophilic interior of the αHL pore provides an energetic barrier to the translocation of hydrophobic peptides. Extending this reasoning, it was proposed that engineering negatively charged aspartic acid residues into the αHL *β*-barrel would reduce the energetic barrier to the transmembrane translocation of positively charged peptides.[52] Indeed, it was found that the incorporation of two rings of acidic residues at both the entrance and the exit of the *β*-barrel increased the rates of peptide association and dissociation. Movileanu and co-workers later exploited the same negatively charged αHL mutants to assemble a protein-protein complex between the αHL nanopore and the 110-amino acid protein barnase.[48] By fusing positively charged peptide fragments to the *N*-terminus of the barnase sequence, the protein could be trapped electrostatically within the lumen of the negatively charged αHL pore (Figure 13A). A series of mutations to the proteins facilitated a systematic investigation of protein-protein interactions at the single-molecule level.

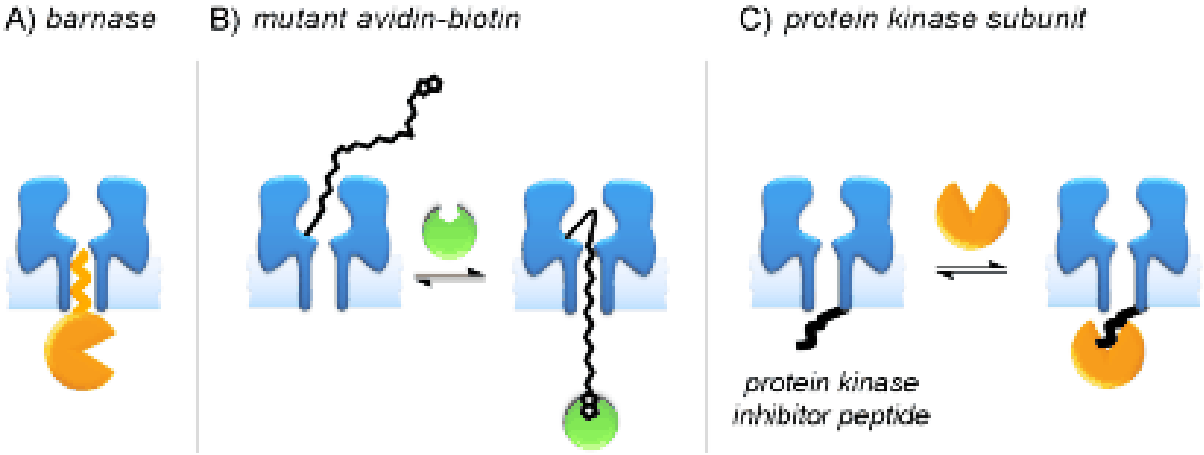

Figure 13. Nanopore-based single-molecule studies of protein interactions. A) Engineered α-haemolysin nanopore and pb2-barnase protein.[49] B) Reversible binding of a mutant streptavidin to the biotin probe can be detected by using ion current recordings.[50] The PEG linker is terminated with a biotin group and covalently tethered to a mutant cysteine residue within the α-haemolysin pore. C) Nanopore modified with a protein kinase inhibitor peptide for the detection of kinase binding.[51, 52]

Researchers have developed a number of different nanopore-based approaches for detecting protein binding. For example, the biotin-terminated oligonucleotides discussed earlier have been exploited in the detection of avidin/streptavidin binding (Figure 6A to 6B).[2] In the absence of streptavidin, a ssDNA probe may freely translocate through the pore causing short-lived current blockades. However, in the presence of streptavidin long current blockades were observed. The concentration of these biotin-binding proteins could be measured because the ratio of short-lived to long-lived blockades is proportional to the concentration of streptavidin when excess biotinylated DNA was present. Bayley and co-workers have engineered nanopore detectors for streptavidin by covalently attaching a biotinylated polyethylene glycol (PEG) chain inside the lumen of the αHL pore (Figure 13B).[49] The device was able to detect the reversible binding of single molecules of a mutant streptavidin on either side of the bilayer since the flexible 3.4 kDa polymer was free to traverse both sides of the bilayer. Binding events were detected as the decrease in the ion current passing through the pore on the sub-millisecond timescale.

Extending these studies, Bayley and co-workers employed two different strategies to assemble a detector for a specific protein kinase enzyme. In the first study, a short PEG linker was used to attach a peptide inhibitor to the trans-entrance of the αHL pore, and in a follow-on study the same peptide inhibitor was genetically encoded within the sequence of one of the αHL monomers (Figure 13C).[50, 51] When the catalytic subunit of cAMP-dependent protein kinase was bound to the inhibitor peptide attached to the αHL pore, a partial blockage of the ion current was observed, allowing the detection of binding events at the single-molecule level. The kinetic and thermodynamic parameters for the binding events were determined and compared well with ensemble measurements.

4.3 Examining nucleic acid-manipulating proteins

Nucleic acid-binding and manipulating proteins are exciting subjects within the field biophysics due to their essential roles in the maintenance and regulation of the genome. Nanopore-based approaches are able to complement existing single-molecule methods to reveal new information about the interactions and mechanisms of these intriguing proteins.

Kasianowicz and co-workers examined the binding of bromodeoxyuridine polyclonal antibody to ssDNA terminated with a single bromodeoxyuridine base using αHL (Figure 14A).[2] Upon addition of the antibody, long current blockades were observed due to capture of the DNA•antibody complex in the nanopore.

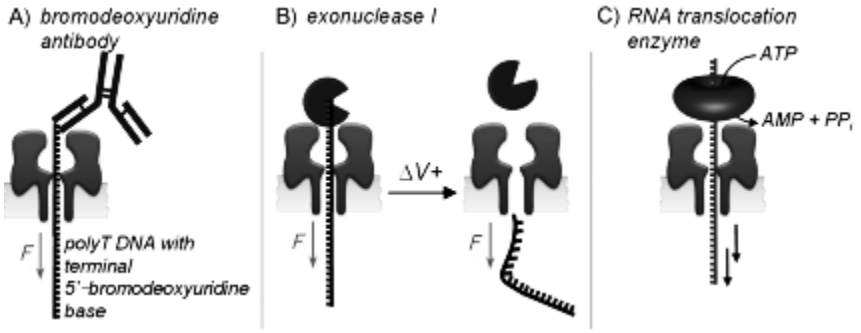

Figure 14. Nanopore detection of DNA–protein interactions. A) Binding of bromodeoxyuridine antibody to bromodeoxyuridine DNA in nanopore experiments.[2] B) Study of ssDNA–exonuclease I complexes.[53] C) Detection of viral RNA translocation enzyme ATPase P4 by using an α-haemolysin detector.[54]

Recently, Akeson and co-workers used nanopore detection to study the interaction of ssDNA with exonuclease I (exo I) (Figure 14B).[53] The blockage current *vs.* dwell time signatures contained two clusters of events, one corresponded to free ssDNA, and the other to the ssDNA•exo I complexes. The rate of ssDNA translocation was reduced when the enzyme was bound to the ssDNA. Furthermore, single ssDNA•exo I complexes could be pulled apart by increasing the magnitude of the applied electric field. In this way, the ion current traces could be used to probe the dissociation rate of the complexes in a similar manner to earlier nanopore-based investigations of DNA unzipping (Figures 3 and 6).

ATPase P4 is a viral RNA packaging motor protein from bacteriophage ϕ8 that couples ATP hydrolysis to movement along RNA and has also been studied using αHL. More specifically, researchers used a nanopore detector to examine the reversible association of RNA•P4 enzyme complexes at single-molecule level (Figure 14C).[54] The oligoribonucleotide 5'-$C_{25}A_{25}$-3' was recorded during its passage through αHL, giving rise to current blockades with an average duration of 0.5 ms. After the addition of ATPase P4 much longer translocation events of between 10-1000 ms were observed, which were attributed to capture of enzyme-RNA complexes. The addition of ATP resulted in the disappearance of these long-duration events, suggesting the rapid dissociation of the RNA•enzyme complexes. The frequency of events was also dependent on the P4 enzyme concentration and the oligoribonucleotide length, which was consistent with the mechanism of ATP-dependent RNA translocation. The rate of dissociation of the RNA•enzyme complexes was found to be dependent upon the force generated by the externally applied electric field, facilitating the study of the complexes under non-equilibrium conditions.

DNA polymerases are fascinating enzymes that have an essential role in the replication and propagation of genetic information. A series of papers by Akeson, Lieberman and co-workers used nanopore detection to study the substrate binding dynamics of the Klenow Fragment from *E. coli* DNA polymerase I (Figure 15).[55-57] DNA hairpins terminated at their 3'-ends with dideoxynucleotides were captured under an applied potential in the nanopore. DNA polymerase enzymes were able to bind to these hairpins but the 3'-dideoxy-modification prevented the DNA polymerase from extending the DNA by incorporating deoxynucleotide triphosphates (dNTPs). Thus, ion current signatures and dwell times could be used to distinguish between the unbound hairpin (Figure 15A), the binary DNA•polymerase complex (Figure 15B), and the ternary DNA•polymerase•dNTP complexes (Figure 15C). Most strikingly of all, it was possible to identify whether a correctly templated, or a mismatched dNTP molecule was bound within the catalytic site of the individually captured DNA•polymerase complexes. Further insights into the mechanism of dNTP recognition by the DNA polymerase were gained when it was found that the dwell times of the ternary DNA•polymerase•dNTP complexes depended heavily on the presence of Mg^{2+} ions.[55] Later, real-time partitioning of dNTPs into and out of captured DNA•polymerase complexes was reported.[56] Adoption of a DNA rotaxane approach (similar to that shown in Figure 6) combined with precise, high-speed voltage control has also allowed rapid interrogation of DNA•polymerase complexes.[57]

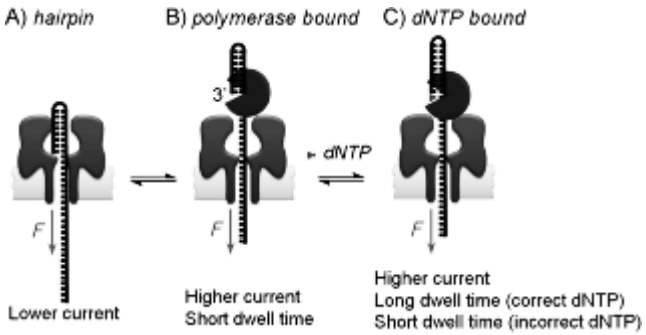

Figure 15. DNA polymerase–DNA binding and deoxynucleotide triphosphate dependence have been investigated by using nanopores.[55–57]

In section 3.3 we introduced a supramolecular nanopore-rotaxane complex developed by Ghadiri and co-workers with the ability to measure the length of single molecule of DNA with single-base precision (Figure 8).[35] This device was configured such that the dsDNA region served as a primer-template complex containing a 3-OH' group onto which the templated addition of nucleotides could be catalysed by DNA polymerase. The device was then cycled between a 'monitoring mode', in which the length of the DNA primer molecule was measured with single-base accuracy, and an

'extension mode' in which the dsDNA primer template complex was fully exposed to activity of the enzyme.

Incorporation of a single base increased the ratio of DNA to PEG threaded through the channel resulting in stepwise increases in the ion current flowing through the channel (Figure 16). By using this method it was possible to resolve nine consecutive single-nucleotide primer extension steps and it is believed to be the first single-molecule method to resolve DNA polymerase activity with single-base precision.[35]

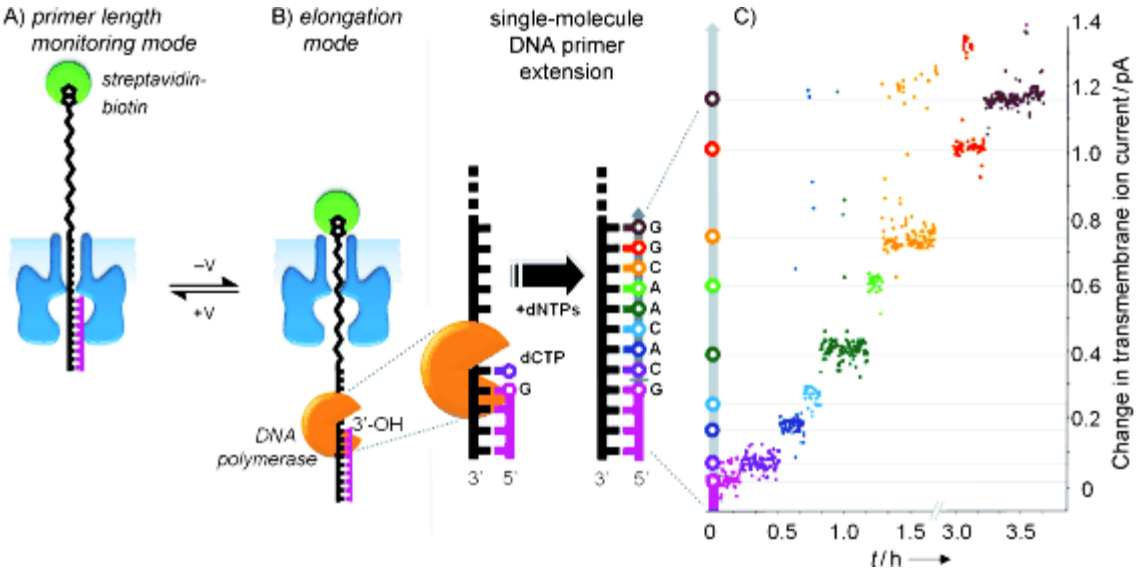

Figure 16. Monitoring DNA polymerase-catalysed extension of a single DNA primer molecule with single-nucleotide resolution by using a nanopore-based device.[35] A) The double-stranded DNA region and the streptavidin cap serve as stoppers trapping the threaded DNA–PEG copolymer in place. B) DNA primer extension by DNA polymerase in the elongation mode results in the section of the ssDNA that was blocking the pore being replaced by an equal length of PEG polymer. This process can be monitored by using ion current recordings in the primer length monitoring mode (A). C) Because the PEG polymer blocks the ion current flowing through the pore less than the DNA, the base-by-base extension of a single molecule of DNA by DNA polymerase can be monitored from the corresponding stepped increases in the current.

5. Summary & Outlook

From its origins in the field of electrophysiology, the development of nanopore-based methods was initially spurred on by the prospect of sequencing single DNA molecules using α-haemolysin. The

construction of nanopore-based devices that have been engineered to a particular task has enabled researchers to innovate and broadened their horizons in to the wider field of biophysics, where there has been an abundance of achievements. The structure and interactions of oligonucleotides, peptides and proteins have been probed extensively. Whilst some of the most exciting developments have provided insights into the function and dynamics of complicated biological processes at the single-molecule level. Continued advances in nanopore-based techniques will continue to provide valuable contributions to biophysics, and the emerging fields of nanobiotechnology and synthetic biology.

References

[1] A. N. Kapanidis, T. Strick, *Trends Biochem. Sci.* **2009**, *34*, 234-243.

[2] J J. J. Kasianowicz, S. E. Henrickson, H. H. Weetall, B. Robertson, *Anal. Chem.***2001**, *73*, 2268-2272.

[3] H. Bayley, P. S. Cremer, *Nature* **2001**, *413*, 226-230.

[4] H. Bayley, O. Braha, L.-Q. Gu, *Adv. Mat.* **2000**, *12*, 139-142.

[5] D. Branton, D. W. Deamer, A. Marziali, H. Bayley, S. A. Benner, T. Butler, M. Di Ventra, S. Garaj, A. Hibbs, X. Huang, S. B. Jovanovich, P. S. Krstic, S. Lindsay, X. S. Ling, C. H. Mastrangelo, A. Meller, J. S. Oliver, Y. V. Pershin, J. M. Ramsey, R. Riehn, G. V. Soni, V. Tabard-Cossa, M. Wanunu, M. Wiggin, J. A. Schloss, *Nat. Biotechnol.* **2008**, *26*, 1146-1153.

[6] A. Meller, L. Nivon, D. Branton, *Phys. Rev. Lett.* **2001**, *86*, 3435-3438.

[7] C. Dekker, *Nat. Nanotechnol.* **2007**, 2, 209-215.

[8] R. F. Purnell, K. K. Mehta, J. J. Schmidt, *Nano Letters* **2008**, *8*, 3029-3034.

[9] L. Song, M. R. Hobaugh, C. Shustak, S. Cheley, H. Bayley, J. E. Gouaux, *Science* **1996**, *274*, 1859-1886.

[10] J. Schmidt, *J. Mater. Chem.* **2005**, *15*, 831-840.

[11] P. Mueller, D. O. Rudin, H. T. Tien, W. C. Wescott, *Nature* **1962**, *194*, 979-980.

[12] M. Montal, P. Mueller, *Proc. Nat. Acad. Sci. U. S. A.* **1972**, *69*, 3561-3556.

[13] E. Neher, B. Sakmann, J. H. Steinbach, *Pfluegers Archiv.* **1978**, *375*, 219-228.

[14] D. J. A. Wyllie, *Neuromethods* **2002**, *35*, 69-109.

[15] J. J. Kasianowicz, E. Brandin, D. Branton, D. Deamer, *Proc. Natl. Acad. Sci. U. S. A.* **1996**, *93*, 13770-13773.

[16] A. Meller, L. Nivon, E. Brandin, J. Golovchenko, D. Branton, *Proc. Natl. Acad. Sci.U. S. A.* **2000**, *97*, 1079-1084.

[17] J. Mathe, H. Visram, V. Viasnoff, Y. Rabin, A. Meller, *Biophys. J.* **2004**, *87*, 3205-3212.

[18] S. Winters-Hilt, W. Vercoutere, V. S. DeGuzman, D. Deamer, M. Akeson, D. Haussler, *Biophys. J.* **2003**, *84*, 967-976.

[19] W. A. Vercoutere, S. Winters-Hilt, V. S. DeGuzman, D. Deamer, S. E. Ridino, J. T. Rodgers, H. E. Olsen, A. Marziali, M. Akeson, *Nucleic Acids Res.* **2003**, *31*, 1311-1318.

[20] A. F. Sauer-Budge, J. A. Nyamwanda, D. K. Lubensky, D. Branton, *Phys. Rev. Lett.* **2003**, *90*, 238101/238101-238101/238104.

[21] J. W. Shim, Q. Tan, L.-Q. Gu, *Nucleic Acids Res.* **2009**, *37*, 972-982.

[22] W. Vercoutere, S. Winters-Hilt, H. Olsen, D. Deamer, D. Haussler, M. Akeson, *Nat. Biotechnol.* **2001**, *19*, 681.

[23] S. Neeidle, S. Balasubramanian, *Quadruplex Nucleic Acids*, Royal Society of Chemistry, Cambridge (2006).

[24] M. R. Stratton, P. J. Campbell, P. A. Futreal, *Nature* **2009**, *458*, 719-724.

[25] M. Akeson, D. Branton, J. J. Kasianowicz, E. Brandin, D. W. Deamer, *Biophys. J.* **1999**, *77*, 3227-3233.

[26] T. Z. Butler, J. H. Gundlach, M. A. Troll, *Biophys. J.* **2006**, *90*, 190-199.

[27] J. Mathe, A. Aksimentiev, D. R. Nelson, K. Schulten, A. Meller, *Proc. Nat. Acad. Sci. U. S. A.* **2005**, *102*, 12377-12382.

[28] N. Ashkenasy, J. Sanchez-Quesada, H. Bayley, M. R. Ghadiri, *Angew. Chem.* **2005**, *117*, 1425–1428; *Angew. Chem. Int. Ed.* **2005**, *44*, 1401-1404.

[29] A. Somoza, *Chem. Soc. Rev.* **2008**, *37*, 2668-2675.

[30] J. Nakane, M. Wiggin, A. Marziali, *Biophys. J.* **2004**, *87*, 3618.

[31] D. Stoddart, A. J. Heron, E. Mikhailova, G. Maglia, H. Bayley, *Proc. Natl. Acad. Sci. U. S. A.* **2009**, *106*, 7702-7007.

[32] J. Sanchez-Quesada, A. Saghatelian, S. Cheley, H. Bayley, M. R. Ghadiri, *Angew. Chem.* **2004**, *116*, 3125–3129; *Angew. Chem., Int. Ed.* **2004**, *43*, 3063-3067.

[33] D. B. Amabilino, J. F. Stoddart, *Chem. Rev.* **1995**, *95*, 2725-2829.

[34] E. R. Kay, D. A. Leigh, F. Zerbetto, *Angew. Chem.* **2006**, *119*, 72–196; *Angew. Chem. Int. Ed.* **2007**, *46*, 72-191.

[35] S. L. Cockroft, J. Chu, M. Amorin, M. R. Ghadiri, *J. Am. Chem. Soc.* **2008**, *130*, 818-820.

[36] N. Mitchell, S. Howorka, *Angew. Chem.* **2008**, *120*, 5647–5650; *Angew. Chem. Int. Ed.* **2008**, *47*, 5565-5568.

[37] S. Howorka, S. Cheley, H. Bayley, *Nat. Biotechnol.* **2001**, *19*, 636-639

[38] S. Howorka, L. Movileanu, O. Braha, H. Bayley, *Proc. Nat. Acad. Sci. U. S. A.* **2001**, *98*, 12996-13001.

[39] L. Q. Gu, O. Braha, S. Conlan, S. Cheley, H. Bayley, *Nature* **1999**, *398*, 686-690.

[40] Y. Astier, O. Braha, H. Bayley, *J. Am. Chem. Soc.* **2006**, *128*, 1705-1710.

[41] J. Clarke, H.-C. Wu, L. Jayasinghe, A. Patel, S. Reid, H. Bayley, *Nat. Nanotechnol.* **2009**, *4*, 265-270.

[42] T. C. Sutherland, Y.-T. Long, R.-I. Stefureac, I. Bediako-Amoa, H.-B. Kraatz, J. S. Lee, *Nano Lett.* **2004**, *4*, 1273-1277.

[43] R. Stefureac, Y.-T. Long, H.-B. Kraatz, P. Howard, J. S. Lee, *Biochem.* **2006**, *45*, 9172-9179.

[44] L. Movileanu, J. P. Schmittschmitt, J. M. Scholtz, H. Bayley, *Biophys. J.* **2005**, *89*, 1030-1045.

[45] R. I. Stefureac, J. S. Lee, *Small* **2008**, *4*, 1646-1650.

[46] G. Oukhaled, J. Mathe, A. L. Biance, L. Bacri, J. M. Betton, D. Lairez, J. Pelta, L. Auvray, *Phys. Rev. Lett.* **2007**, *98*, 158101.

[47] R. Stefureac, L. Waldner, P. Howard, J. S. Lee, *Small* **2008**, *4*, 59-63.

[48] M. M. Mohammad, S. Prakash, A. Matouschek, L. Movileanu, *J. Am. Chem. Soc.* **2008**, *130*, 4081-4088.

[49] L. Movileanu, S. Howorka, O. Braha, H. Bayley, *Nat. Biotechnol.* **2000**, *18*, 1091-1095.

[50] H. Xie, O. Braha, L.-Q. Gu, S. Cheley, H. Bayley, *Chem. Biol.* **2005**, *12*, 109-120.

[51] S. Cheley, H. Xie, H. Bayley, *ChemBioChem* **2006**, *7*, 1923-1927.

[52] A. J. Wolfe, M. M. Mohammad, S. Cheley, H. Bayley, L. Movileanu, *J. Am. Chem. Soc.* **2007**, *129*, 14034-14041.

[53] B. Hornblower, A. Coombs, R. D. Whitaker, A. Kolomeisky, S. J. Picone, A. Meller, M. Akeson, *Nat. Methods* **2007**, *4*, 315-317.

[54] Y. Astier, D. E. Kainov, H. Bayley, R. Tuma, S. Howorka, *ChemPhysChem* **2007**, *8*, 2189-2194.

[55] S. Benner, R. J. A. Chen, N. A. Wilson, R. Abu-Shumays, N. Hurt, K. R. Lieberman, D. W. Deamer, W. B. Dunbar, M. Akeson, *Nat. Nanotechnol.* **2007**, *2*, 718-724.

[56] N. Hurt, H. Wang, M. Akeson, K. R. Lieberman, *J. Am. Chem. Soc.* **2009**, *131*, 3772-3778.

[57] N. A. Wilson, R. Abu-Shumays, B. Gyarfas, H. Wang, K. R. Lieberman, M. Akeson, W. B. Dunbar, *ACS Nano* **2009**, *3*, 995-1003.